Submillimeter wave generation and noise in InP diodes

V. Mitin and V. Gruzinskis
Department of Electrical and Computer Engineering, Wayne State University, Detroit, Michigan 48202

E. Starikov and P. Shiktorov
Semiconductor Physics Institute, Vilnius 2600, Lithuania

(Received 16 August 1993; accepted for publication 4 October 1994)

High-frequency (350–750 GHz) generation in submicrometer InP diodes is investigated by modified hydrodynamic and Monte Carlo particle (MCP) techniques. The noise power spectral density P_n in the diode loaded by resistor R and generation spectra P_g in a series resonant RL circuit are calculated using the MCP technique. It is shown that at the biases above the generation threshold the P_n has a peak at the frequency $f_{\max}$ which corresponds to the highest generation frequency at the given R. The excess noise arises in the frequency region where the real part of diode impedance $\mathrm{Re}\,Z$ has negative values. At the bias below the generation threshold (i.e., when $\mathrm{Re}\,Z$ is positive over entire frequency range) the $P_n(f)$ has the usual Lorenzian shape. The MCP simulation of P_g for 0.25-μm-length diode shows the Gaussian shape of the spectra at frequencies 517 and 622 GHz. The P_g broadening at higher frequencies is the result of interaction between the self-oscillations at frequency $f_{\max}$ and circuit-driven oscillations.

I. INTRODUCTION

Solid-state millimeter and submillimeter wave systems (MSWS) are very suitable for the communications and radar applications due to their broad bandwidths, high resolution, small size, light weight, resistance to jamming, and narrow beamwidth for pinpoint tracking. Their adverse weather operation is good compared with that of optical and infrared systems, which exhibit poor penetration characteristic in fog, haze, smoke, and dust. The above characteristics indicate that MSWS technology has major advantages over optical and infrared devices in seeker and detection systems. Millimeter wave systems (frequency range: 30–300 GHz) are relatively well developed. Submillimeter wave (300–3000 GHz) systems are still far from practical realization, due to a lack of high-frequency radiation sources. Therefore, an important task facing high-speed electronics is to increase the cutoff frequencies of such major devices as diodes, transistors, etc.

In recent years, progress in increasing the operating frequency of MSWS has chiefly been through development of transferred electron devices (TED). A recent report describes an n^+-n-n^+ InP TED operating at 272 GHz frequency.[1] High-frequency generation (HFG) in usual TEDs arises due to the Hilsum–Ridley–Wattkins–Gunn effect, which uses the negative differential conductivity (NDC) of the steady-state velocity-field characteristic resulting from the carrier transfer into the upper valleys with larger effective mass. The generation frequency in TEDs depends on the length of the n region. Shorter n regions result in higher generation frequencies. On the other hand, the steady-state NDC in shorter diodes becomes weaker and disappears at near-micrometer lengths, due to electron injection from n^+ regions. Therefore, the usual Gunn effect in short samples is impossible; but, this is not a sufficient reason to say that short diodes cannot be used for microwave generation. Electrons in short diodes drift from the source to the drain contact under highly nonstationary conditions.[2] Under such conditions a HFG mechanism different from the classical Gunn effect can arise.[3] According to this mechanism, the HFG in short diodes arises due to heating and transit time delay, which causes velocity overshoot in space.

Let us suppose that the conditions for the stationary transport of carriers are fulfilled, and that the conduction current $j(z)=n(z)v(z)$ is constant throughout the diode. In this case the spatial decrease of velocity is accompanied by a spatial increase of the carrier concentration $n(z)$, since their product is constant through the diode length. Due to Poisson's equation, the carrier concentration increase leads to an increase in the electric field $E(z)$. Thus, in submicrometer n^+-n-n^+ diodes the velocity decrease, which follows the overshoot, is accompanied by an electric-field increase, i.e., spatial negative differential conductivity (SNDC) appears.

Because of SNDC, certain fluctuations of carrier concentration can grow over time, leading to the formation of an accumulation layer in the diode region with decreasing velocity. Then propagation of the layer toward the anode leads to time variations in the conduction current in the diode, or in the total current in the external circuit. When the layer leaves the diode, redistribution of the electric field inside the diode takes place and leads again to velocity overshoot. Thus the process of layer formation, transport across the diode, and disappearance at the anode takes on a periodic character.

Despite the fact that HFG was predicted 10 years ago, it has still not been properly investigated. This is because the theory of HFG in short structures is extremely complicated. A comprehensive theoretical analysis of carrier transport in these devices is based on a kinetic description of carrier heating and, as a rule, is carried out by Monte Carlo particle (MCP) simulation. For a realistic evaluation of HFG output power and conversion efficiency, it is

 0021-8979/94/75(2)/935/7/$6.00

absolutely necessary to simulate the device operation in the resonant circuit, which consists of discrete elements such as resistance R, inductance L, and capacitance C. Accounting for the external circuit in a MCP simulation is a complicated task. This explains the small number of publications on this problem. To find the maximum operation frequency, output power, or conversion efficiency of given TED in the external circuit, it is necessary to optimize a function which depends on applied voltage U and circuit parameters such as R, L, and C. The Monte Carlo calculations are time consuming, and it is more convenient to use other methods for this purpose. Therefore, we use the modified hydrodynamic (MH) method[4] for the circuit optimization calculations. On the other hand, using the MCP and MH methods for the same problem allows us to check the reliability of the results obtained.

The noise of a microwave generator is an important device characteristic. Noise reduction is often the main problem facing device designers. On the other hand, noise measurements give information about the physical processes in the structure. One of the most reliable and direct theoretical methods for noise investigation is the Monte Carlo method. This method is widely used for the noise simulations in bulk semiconductors and gives a good agreement with available experimental data. The MCP method for noise simulation in n^+-n-n^+ structures was proposed by Zimmerman and Constant.[5] The MCP method is not widely used for the noise investigations in submicron n^+-n-n^+ structures because it needs a great deal of computer time, and, due to the complexity of the investigated objects, problems of interpretation of the obtained results there always arise. Due to strong nonlocal effects, the drift velocity dependence on the electric-field strength for an n^+-n-n^+ structure, especially one of submicrometer size, carries essentially less information than the same dependencies for bulk materials. Each n^+-n-n^+ structure with certain doping profile and geometry should be considered separately. The drift velocity have no clear meaning within such a system. In most cases an artificial description of such a system by drift velocity complicates the interpretation of the results. The most natural and experimentally measurable characteristic of the device is the current-voltage relation. Therefore, for noise calculations by MCP the method[5] most preferable from our point of view is one in which the current and voltage fluctuations are calculated straightforwardly. Unfortunately, this method accounts only for the conduction current fluctuations which are the result of velocity fluctuations. The origin of total current fluctuations is the velocity and concentration fluctuations. The concentration fluctuations manifest themselves through the displacement current. To account for the displacement current we propose to simulate directly the voltage or current (in principal the same) fluctuations in a resistor connected in series with an n^+-n-n^+ structure. Because the current through the resistor is the sum of the conduction and displacement currents, the displacement current fluctuations in the device are naturally accounted for. The noise power calculated in this way can be directly measured by experiment. Using this modified method, we can investigate not only the noise in the structure but the generation spectra in the resonant circuit as well.

In this article we present the results of HFG investigations in submicron InP diodes by both MH and MCP methods. The diode impedance, generated microwave power, and microwave power conversion efficiency are calculated. The noise power spectral density in the diode loaded by resistor R and generation spectra in a series resonant RL circuit are calculated. The external resonant circuit is considered in both MH and MCP simulations. A comparison is made between the results obtained by the different methods.

II. SIMULATION METHODS

A. Monte Carlo particle

The calculations of electron transport in n^+-n-n^+ InP structure are carried out by simultaneous solution of Boltzmann and Poisson equations. The electron scattering by phonons and ionized impurities is simulated by the Monte Carlo technique in three-dimensional momentum space. The three-valley InP model[6] is used in the simulation. The Poisson equation is solved in the direction of the applied electric field using a charge-sheet method.[7,8] The electrons in this algorithm are represented by negatively charged sheets that easily penetrate each other. The advantage of the given method is that we do not need a spatial mesh for the field distribution calculation. The value of the field for every single sheet is calculated without any interpolating formulas. This permits an accurate allowance for the large gradients of the electric field in the contact region. The length and doping density of $n+$ regions are chosen high enough so that displacement currents at the simulation space boundaries are negligible compared with the total current density in the structure. In view of the fact that in such conditions the quasineutrality of the space charge in the simulation region is conserved, the particles crossing either end of the structure are reinjected from the other end with the same components of momentum. The time step, which depends on applied voltage, varies from 1 to 2.5 fs. The number of charge-sheets varies from 5000 to 10 000.

The RL circuit, consisting of series connected load resistance R, inductance L, and the diode, is accounted for in MCP simulation by the second-order differential equation for the bias U_d on the diode,

$$LC_0\frac{d^2U_d}{dt^2}+RC_0\frac{dU_d}{dt}+U_d=U_a-L\frac{dj_{\text{cond}}}{dt}-Rj_{\text{cond}}, \tag{1}$$

where $C_0=\kappa\kappa_0/d$, κ is the dielectric permittivity, κ_0 is the dielectric constant, d is the full length of simulation region, U_a is the constant voltage applied to the circuit, and j_{cond} is a conduction current density. Setting $L=0$ in Eq. (1), the equation for the diode loaded only by resistor R (i.e., for a diode placed in an R circuit) can be obtained:

$$RC_0\frac{dU_d}{dt}+U_d=U_a-Rj_{\text{cond}}. \tag{2}$$

The noise $P_n(f)$ and generation $P_g(f)$ power spectral densities, where f is the frequency, are calculated by analyzing the voltage fluctuations on load resistance R. For this purpose the voltage-voltage correlator is calculated:

$$K_u(\tau)=\frac{1}{T}\int_0^T U_R(t)\,U_R(t+\tau)dt, \tag{3}$$

where T is the length in time units of the voltage $U_R(t)$ on R trajectory in a stationary condition and τ is a delay time. The $P_n(f)$ and $P_g(f)$ are calculated in the standard way,

$$P_{n,g}(f)=\frac{4}{R}\int_0^\infty K_u(t)\cos(2\pi ft)dt. \tag{4}$$

Defined by Eq. (21), P_n and P_g are the power density generated by the diode with unit cross-section area in the load resistor R, which is given in units of $\Omega\ \mathrm{m}^2$.

B. Modified hydrodynamic

A modified hydrodynamic model[4] is based on the velocity and energy conservation equations in the single electron gas approximation,

$$\frac{\partial n}{\partial t}=-\frac{\partial}{\partial z}(n\upsilon), \tag{5}$$

$$\frac{\partial \upsilon}{\partial t}=eEm^{-1}-\nu_\upsilon\upsilon-\upsilon\frac{\partial \upsilon}{\partial z}-\frac{1}{n}\frac{\partial}{\partial z}(nQ_\upsilon), \tag{6}$$

$$\frac{\partial \mathscr{E}}{\partial t}=eE\upsilon-\nu_{\mathscr{E}}(\mathscr{E}-\mathscr{E}_{\mathrm{th}})-\upsilon\frac{\partial \mathscr{E}}{\partial z}-\frac{1}{n}\frac{\partial}{\partial z}(nQ_{\mathscr{E}}), \tag{7}$$

where e is the electron charge, υ is the drift velocity, E is the electric-field strength, n is the electron concentration, $\mathscr{E}$ is the mean energy ($\mathscr{E}=\langle\epsilon\rangle$), and $\mathscr{E}_{\mathrm{th}}$ is the carrier thermal energy. The MH contains five parameters which depend only on $\mathscr{E}(z,t)$ and can be easily obtained from the Monte Carlo simulation of the space homogeneous and stationary hot-electron system,

$$m^{-1}=\left\langle\frac{\partial^2\epsilon}{\partial p^2}\right\rangle \tag{8}$$

is the reciprocal effective mass of carriers in the electric field direction,

$$\nu_\upsilon=\frac{eE\langle m^{-1}\rangle}{\langle\upsilon\rangle} \tag{9}$$

and

$$\nu_{\mathscr{E}}=\frac{eE\langle\upsilon\rangle}{\langle\epsilon\rangle-\mathscr{E}_{\mathrm{th}}} \tag{10}$$

are the velocity and energy relaxation rates, respectively,

$$Q_\upsilon=\langle\upsilon^2\rangle-\langle\upsilon\rangle^2 \tag{11}$$

is the variance of velocity fluctuations in the electric-field direction,

$$Q_{\mathscr{E}}=\langle\upsilon\epsilon\rangle-\langle\upsilon\rangle\langle\epsilon\rangle, \tag{12}$$

is the covariance of velocity and energy fluctuations, υ and ϵ are the electron instant velocity and energy, respectively, and brackets have the meaning of average over the electron distribution in the momentum space.

For the solution of the Poisson equation, the electric-field distribution in n^+-n-n^+ structure is given in the form

$$E(z,t)=E(0,t)+\frac{e}{\kappa\kappa_0}\int_0^z[n(z,t)-N_D(z)]dz, \tag{13}$$

where N_D is the ionized donor concentration. The electric field at $z=0$ was calculated from the condition

$$U_d(t)=\int_0^d E(z,t)dz. \tag{14}$$

Equation (5)–(14) allow us to simulate the diode in voltage-driven regime. In the current-driven regime, the voltage $U_d(t)$ depends on total current

$$j_{\mathrm{tot}}(t)=j_{\mathrm{cond}}(t)+j_{\mathrm{disp}}(t), \tag{15}$$

where

$$j_{\mathrm{cond}}(t)=\frac{e}{d}\int_0^d n(z,t)\upsilon(z,t)dz, \tag{16}$$

is the conduction current density and

$$j_{\mathrm{disp}}(t)=C_0\frac{d}{dt}U_d(t), \tag{17}$$

is the displacement current. Combining Eqs. (15)–(17) it is easy to obtain the equation for voltage in the current-driven regime,

$$\frac{d}{dt}U_d(t)=\frac{1}{C_0}[j_{\mathrm{tot}}(t)-j_{\mathrm{cond}}(t)]. \tag{18}$$

To account for a series resonant RL circuit it is necessary to add the equation for total current,

$$\frac{d}{dt}j_{\mathrm{tot}}(t)=\frac{1}{L}[U_a-Rj_{\mathrm{tot}}(t)-U_d(t)]. \tag{19}$$

It is well known that TED's cannot generate in the circuit with sufficiently high resistance R. Therefore, the current-driven regime is most suitable for the diode impedance calculation at any point of the current-voltage relation if it has no static NDC. This is because the voltage oscillations are damped by the internal infinite resistance of current source. The impedance spectrum in the current-driven regime can be calculated according to the expression

$$Z(\omega)=\int_0^\infty D_u\exp(-i\omega t)dt, \tag{20}$$

where $\omega=2\pi f$ and

$$D_u(t)=\frac{1}{\Delta j_{\mathrm{tot}}}\frac{d}{dt}U_d(t) \tag{21}$$

is the aftereffect function where $U_d(t)$ is diode voltage transient response on the small steplike current variation Δj_{tot} switched on at $t=0$.

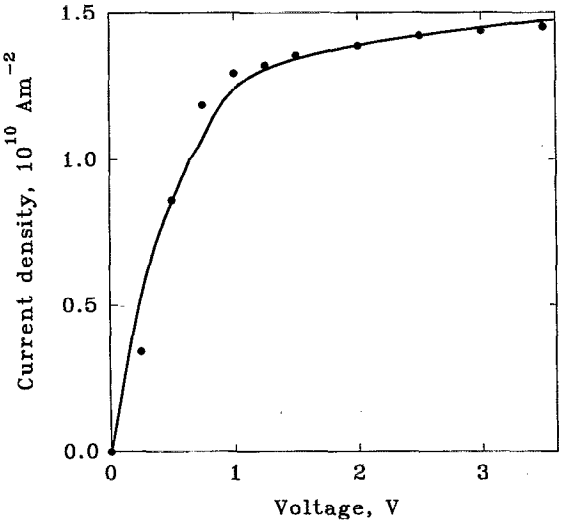

FIG. 1. Current-voltage relation of n^+-n-n^+InP structure. The length of the n region is 0.25 μm, and the doping concentration in the n and n^+ regions is 2×10^{17} and 3×10^{18} cm^{-3}, respectively. The relation is obtained by two different methods: MH (solid line) and MCP (solid circles) simulations.

III. RESULTS AND DISCUSSION

In our simulation, the following parameters of n^+-n-n^+InP are chosen: the length of the n region is 0.25 μm, and the doping concentration in the n and n^+ regions is 2×10^{17} and 3×10^{18} cm^{-3}, respectively. These parameters result in the highest available frequency with reasonable conversion efficiency[9] at the lattice temperature $T=300$ K. The calculated current-voltage relation is shown in Fig. 1. Dots correspond to the MCP simulation, and the solid line represents MH calculations. As one can see, the results of both calculations coincide and there is no region with static negative differential conductivity in this current-voltage relation. However, the linear analysis carried out by the MH method in the current-driven regime shows the presence of dynamic NDC above the voltage $U=1.1$ V. In particular, at $U=3$ V (see Fig. 2) the NDC exists in the frequency range from 350 up to 1050 GHz with a maximum value 3.6×10^{-10} Ω m^2 at 520 GHz. The MCP simulation in the RL circuit shows a conversion efficiency at 520 GHz as high as 1.85%. The load resistance R chosen to obtain maximum efficiency was 10^{-10} Ω m^2, and the average voltage drop on the diode was about 3 V. With increasing operating frequency, which is driven by the inductance L, the efficiency falls, and at 750 GHz it was only 0.4%. Figure 3(a) shows the conversion efficiency's dependence on generation frequency. The MCP and MH calculations agree qualitatively with each other. The same agreement was obtained in the case of generation power dependence on frequency [see Fig. 3(b)]. As follows from Fig. 3(b) the diode with a crossection area 100 μm^2

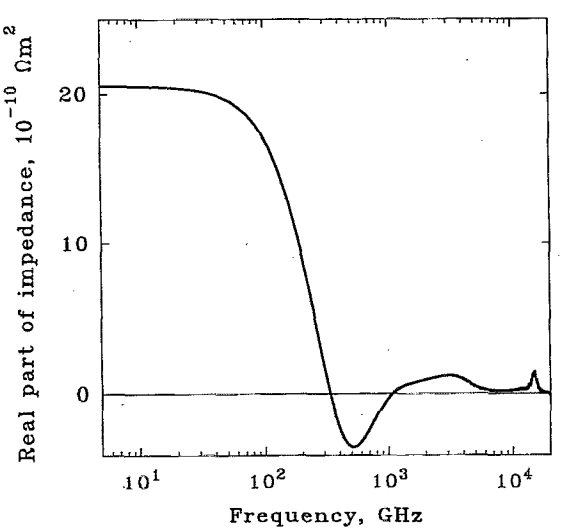

FIG. 2. Dependence of real part of impedance on frequency. The structure parameters are the same as in Fig. 1. MH simulation.

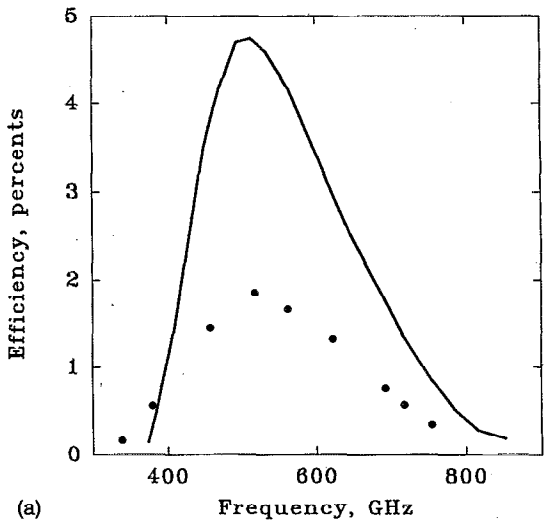

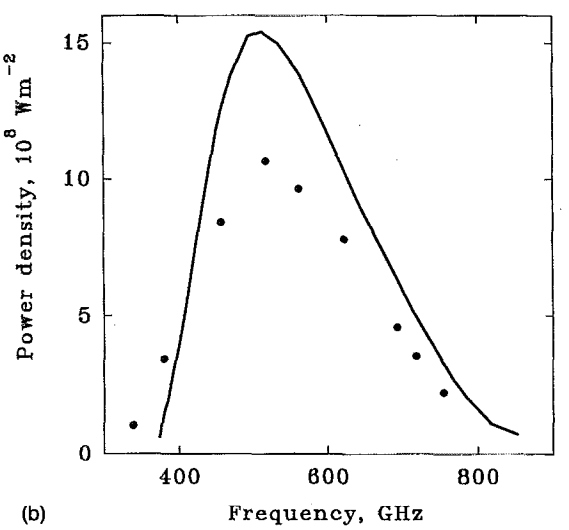

FIG. 3. Dependence of (a) microwave power conversion efficiency and (b) microwave power density on frequency. The structure parameters are the same as in Fig. 1. MH (solid line) and MCP (solid circles) simulations.

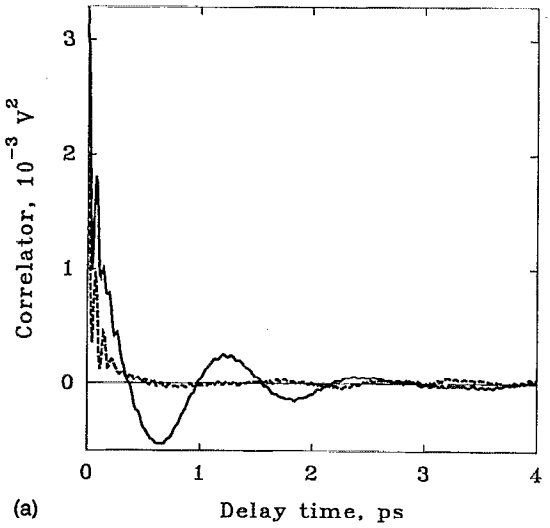

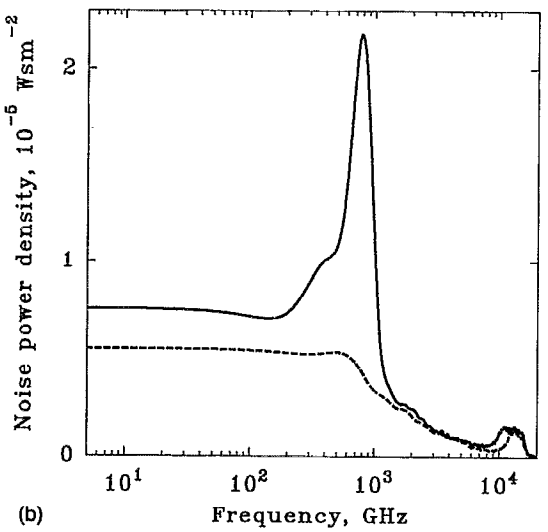

FIG. 4. (a) Voltage-voltage correlation functions and (b) noise power spectral densities in R circuit at two different diode biases: $U_d=1$ V (short dashes) and $U_d=3$ V (solid). The structure parameters are the same as in Fig. 1. Load resistance $R=10^{-10}$ Ω m^2. MCP simulation.

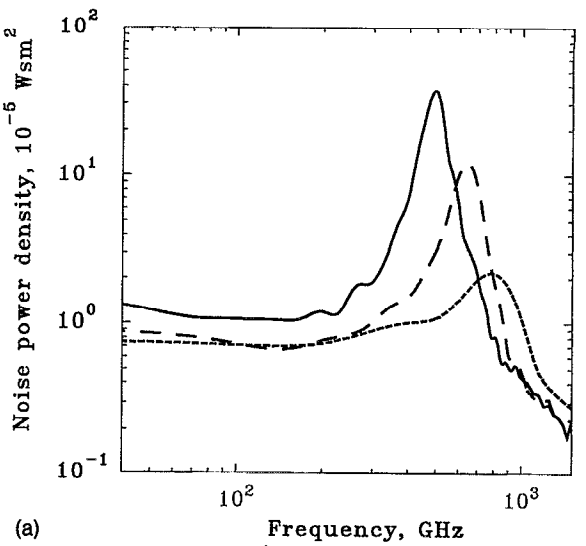

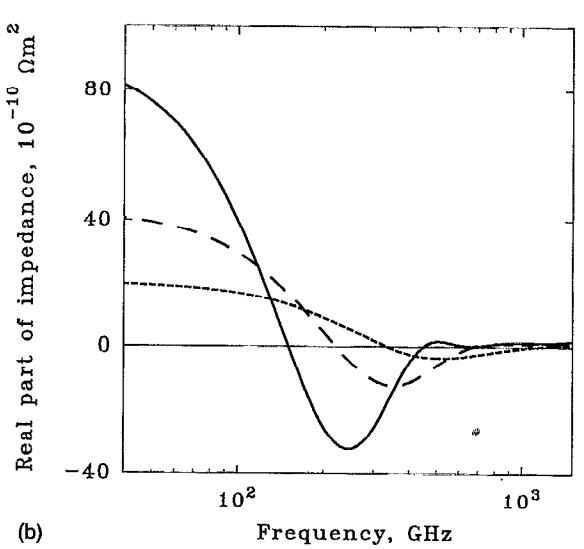

FIG. 5. (a) Noise power spectral density and (b) real part of impedance vs frequency in R circuit. The length of n regions is 0.25 μm (short dashes), 0.4 μm (dashes), 0.6 μm (solid). Other structure parameters are the same as in Fig. 1. The diode bias $U_d=3$ V. Load resistance $R=10^{-10}$ Ω m^2. (a) MCP and (b) MH simulation.

can generate microwave powers of 100 mW at 500 GHz and 20 mW at 750 GHz. These power values are more than sufficient for most practical applications.

The noise and diode generation spectra were investigated by the MCP method. The correlation functions K_U and diode noise power spectral densities P_n are calculated according to Eqs. (3) and (4), respectively. The noise was simulated in a diode loaded by $R=10^{-10}$ Ω m^2. The K_U and P_n for two different values of $U_d=1$ (dashed line) and 3 V (solid line) are shown in Figs. 4(a) and 4(b), respectively. At $U_d=1$ the real part of impedance Re Z is positive in all frequency range. Therefore, the P_n has the usual Lorenzian shape. The high-frequency noise in this case can be related to the shot noise due to the carrier flight from source to drain. At $U_d=3$ V, the noise power spectral density P_n has a maximum in the frequency range where Re Z is negative [compare Figs. 2 and 4(b)]. This is due to the self-excitation of generation in the circuit. The most powerful generation arises when the condition Re $Z+R=0$ is satisfied. To check this assumption, the dependence of P_n on the length of the n region is calculated. Other parameters of the structure remain unchanged. The U_d in this case is equal to 3 V. In Fig. 5(a) the P_n are shown for the lengths of the n region 0.25 (short dashes), 0.4 (dashed), and 0.6 (solid) micrometers. The same is shown for the Re Z in Fig. 5(b). Comparison of Fig. 5(a) with Fig. 5(b) shows that the frequencies of P_n maxima coincide well with the upper frequency limits of negative Re Z. The noise power is enhanced in the frequency range where the Re Z is negative. The negative values of Re Z increase with increasing length of n region [see Fig. 5(b)]. As consequence, the noise power also increases [see Fig. 5(a)]. Therefore, the P_n maxima arise due to the self-excitation of generation.

The integral microwave power P generated in the LR

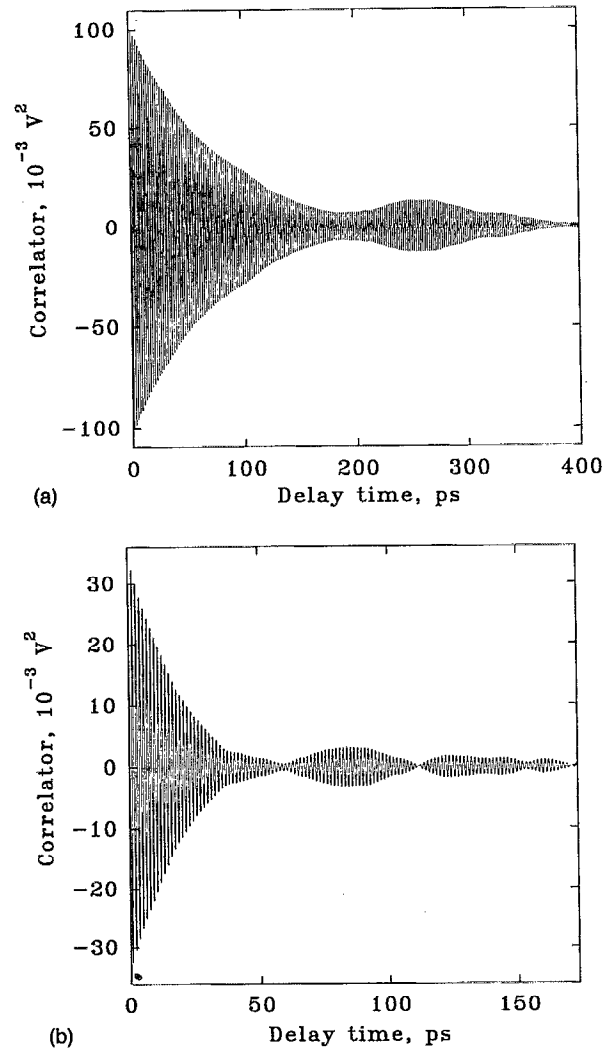

FIG. 6. Voltage-voltage correlation functions in LR circuit at two different inductance values: (a) $L=10^{-22}$ H m^2, and (b) 4×10^{-23} H m^2. The structure parameters are the same as in Fig. 1. The diode bias averaged over the oscillation period $U_d=3$ V, load resistance $R=10^{-10}$ Ω m^2. MCP simulation.

circuit has a maximum at the frequency where the negative Re Z is highest [compare Figs. 2 and 3(b)], while the noise power spectral density $P_n(f)$ of the same structure has a maximum at the upper frequency limit of the negative Re Z values [Figs. 2 and 4(b)]. The P has a maximum at 500 GHz, while the $P_n(f)$ maximum is at approximately 800 GHz. The origin of the microwave power generation in the LR circuit and of the enhanced noise power in the R circuit is the same. The difference is that in the LR circuit the generation proceeds in a nonlinear regime due to the feedback realized through the inductance L, while the excess noise in the R circuit is due to the linear generation regime. In both cases the periodic formation and traveling of accumulation layers is present. In the R circuit the length of the path traveled by a layer is minimal compared with that in the LR circuit, because the strong field necessary for layer nucleation is concentrated near the drain in the case of the R circuit. In the LR circuit the voltage on the diode periodically changes due to L feedback. It causes the drastic changes in field distribution, so that long traveling paths of the layer become available, which results in the lower generation frequencies.

The generated power spectral density $P_g(f)$ in the LR circuit at certain values of L is calculated in the same way as $P_n(f)$. The structure and circuit parameters are the same as for the power and efficiency calculations (Fig. 3). The calculations are performed for three values of $L=10^{-22}$, 6×10^{-23}, and 4×10^{-23} H m^2. The correlators $K_U(t)$ for $L=10^{-22}$ and 4×10^{-23} H m^2 are shown in Figs. 6(a) and 6(b), respectively. It must be pointed out that these calculations are time consuming because the correlation between the voltage oscillations vanishes very slowly in time. For the calculation of $K_U(t)$ shown in Fig. 6(a), a trajectory of the voltage on resistance $U_R(t)$ as long as 6000 ps is necessary. The time step in these calculations did not exceed 2.5 fs. The spectral densities $P_g(f)$ are presented in Fig. 7. The central maxima frequencies of $P_g(f)$ for $L=10^{-22}$, 6×10^{-23}, and 4×10^{-23} H m^2 are $f_0=517$, 622, and 718 GHz, respectively. The narrowest peak is at frequency $f_0=517$ GHz. At 622 GHz the peak is wider. Finally, at 718 GHz we have three well-defined maxima of approximately the same order of amplitude. The broadening of the spectrum at 718 GHz is the result of interaction between the self-oscillations and circuit-driven oscillations. From the above analysis it can be concluded that the maximum noise power spectral density $P_n(f)$ is at the frequency which corresponds to the highest generation frequency f_{max} at a given value of load resistance R [compare Figs. 3(b) and 4(b)]. The optimal generation frequency f_{opt} can be significantly lower. In the case considered here f_{opt} is of about 500 GHz, which is 300 GHz below the f_{max}.

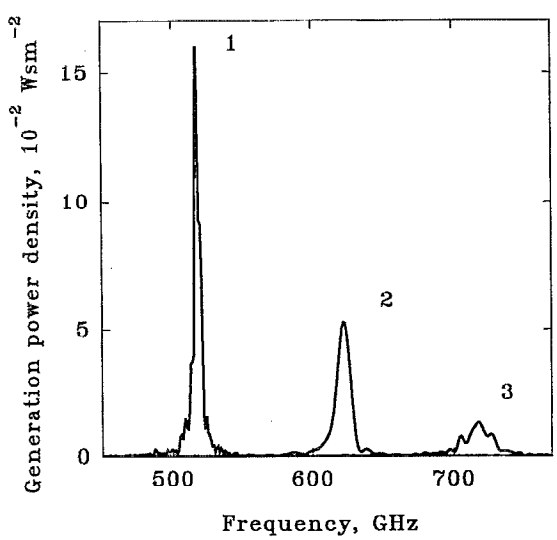

FIG. 7. Generation power spectral density dependencies on frequency in LR circuit. The structure parameters are the same as in Fig. 1. The diode bias averaged over the oscillation period $U_d=3$ V, load resistance $R=10^{-10}$ Ω m^2. The values of inductances are 1: $L=10^{-22}$ H m^2; 2: 6×10^{-23}; 3: 4×10^{-23} H m^2. MCP simulation.

IV. CONCLUSIONS

Previous hydrodynamic simulation results on high-frequency microwave power generation in GaAs and InP submicron diodes[9] are confirmed for InP diodes by Monte Carlo particle simulation. The 0.25-μm-length InP diode loaded by series resonant LR circuit can generate microwave power in wide frequency range from 350 up to 750 GHz. The generation frequency in this frequency range can be tuned by inductance L. The most powerful and efficient generation can occur at frequencies around 500 GHz. The diode with a crossection area of 100 μm^2 can generate microwave power 100 mW at 500 GHz, with a conversion efficiency as high as 1.8%.

Noise power spectral densities were calculated by the MCP technique for different bias values. At the bias below the generation threshold (i.e., when the real part of the impedance is positive over entire frequency range) the noise power spectral density $P_n(f)$ has the usual Lorenzian shape. High-frequency noise in the case of submicron diodes can be related to the shot noise due to the carrier flight from source to drain. The $P_n(f)$ at the biases above the generation threshold has a maximum at a frequency which corresponds to the microwave power generation upper frequency limit at a the given value of load resistance. This excess noise is the result of the self-excitation of generation in the diode, because it appears in the frequency range where the real part of impedance is negative.

The MCP simulation of generation spectra in the RL circuit shows no upper or lower harmonic of the generated signal. The Gaussian shape of the spectra for a 0.25-μm-length diode at frequencies of 517 and 622 GHz indicates that a nearly harmonic output signal is generated. This means that the series RL circuit is optimal for the n^+-n-n^+ InP structure investigated.

[1] A. Rydberg, IEEE Electron Device Lett. **EDL-11**, 439 (1990).
[2] M. P. Shaw, V. Mitin, E. Schöll, and H. Grubin, *The Physics of Instabilities in Solid State Electron Devices* (Plenum, New York, 1992), p. 467.
[3] M. R. Friscourt, P. A. Rolland, A. Cappy, E. Constant, and G. Salmer, IEEE Trans. Electron Devices **ED-30**, 223 (1983).
[4] V. Gruzinskis, E. Starikov, and P. Shiktorov, Solid-State Electron. **36**, 1055 (1993).
[5] J. Zimmerman and E. Constant, Solid-State Electron. **23**, 915 (1980).
[6] Brenan and K. Hess, Solid-State Electron. **27**, 347 (1984).
[7] O. C. Eldridge and M. Feix, Phys. Fluids **5**, 1076 (1962).
[8] V. Gruzinskis and A. Reklaitis, Semicond. Sci. Technol. **3**, 754 (1988).
[9] V. Gruzhinskis, E. Starikov, P. Shiktorov, L. Reggiani, M. Saraniti, and L. Varani, Appl. Phys. Lett. **61**, 1456 (1992).